22

Climate diagnostics by adjoint modelling: A feasibility study.

From: Blessing, S., K. Fraedrich, and F. Lunkeit, 2004: Climate Diagnostics by Adjoint Modelling: A Feasibility Study. *The KIHZ project: Towards a Synthesis of Holocene Proxy Data and Climate Models*, Fischer, H., Kumke, T., Lohmann, G., Flöser, G., Miller, H., von Storch, H., and Negendank, J. F. W., eds. Springer, Berlin Heidelberg New York, 383-396.

Please note: the page numbering in this document only roughly corresponds to the printed version!

Summary. Reconstructing past climate states requires the identification of the mean and the variability of the atmosphere and, once interpreted as a response, the type of the underlying atmospheric forcing. Adjoint modelling diagnostics based on a primitive equations simplified global circulation model (GCM) is used to analyse the climate mean induced by a stormtrack and the variability of a low frequency pattern resembling the North Atlantic Oscillation (NAO). First, given the climate mean, the associated location, shape and intensity of the forcing can be successfully determined so that, rerunning the model with the reconstructed forcing, the original climate variability is retained. Second, given the climate variability represented by a daily NAO-type index, its temperature forcing on short timescales is diagnosed in terms of temperature sensitivity patterns at different time lags. These two feasibility studies of adjoint technique applications demonstrate their potential usefulness in climate and palaeoclimate diagnostics.

22.1 Introduction

For simulations of past climate with general circulation models (GCM) it is important to know, how strong the link between the forcing and the climate response patterns is. Do fixed boundary conditions lead to non-stationary behaviour? Can different conditions generate the same climate? This is of relevance, if circulation patterns deduced form proxy data are simulated as a response to a forcing, which needs to be determined (von Storch *et al.* 2000, Jones and Widmann 2004). This is of particular interest for regional climate change analysis.

The North Atlantic-European sector is dominated by the North Atlantic Oscillation (NAO). It characterises the North Atlantic stormtrack intensity through the pressure difference between Iceland and the Azores. For past climates, Greenland ice core analyses suggest that there is a fundamental change between regionally more active and passive NAO-phases lasting for decades (Appenzeller *et al.* 1998). These two phases can be distinguished by the coupling strength between the NAO and the Pacific-North-American pattern (PNA), which has substantial impact on the continental European climate. Raible *et al.* (2001) show that comparable phases also appear in a purely atmospheric model forced by climatological sea surface temperatures (SST), though integrations coupled with ocean dynamics show a more realistic behaviour. Even a simplified GCM with stormtrack induced variability reveals these regimes of decadal variability (Franzke *et al.* 2001). The underlying mechanisms have yet to be identified. Related atmospheric phenomena such as blocking or zonal index changes have been subject to studies with adjoint models. Perturbations that optimally trigger the onset of blocking were studied in a quasi-geostrophic (Oortwijn 1999) or two-layer primitive equations model (Li *et al.* 1999). Li and Ji (1997) describe an adjoint method to derive forcing modes for a damped barotropic model the response to which is primarily composed of teleconnection patterns.

This paper presents a feasibility study diagnosing the relationship between forcing and climate by adjoint modelling. The model used is the simplified atmospheric circulation model (PUMA, Portable University Model of the Atmosphere, Fraedrich *et al.* (1998)) which represents the dynamical core of a primitive equation GCM forced by linear relaxation processes. Instead of the traditional analysis of the atmospheric response to forcing (like regional diabatic heating of varying intensity), we prescribe the atmosphere's response, say a circulation pattern obtained from proxy data, to determine the underlying forcing, its intensity, and spatial structure. Two cases are distinguished:
(a) Given a climate or time mean temperature field from a complex GCM simulation or proxy data as the only information, the diabatic forcing is reconstructed for a model run. Such a goal has been pursued by Lunkeit *et al.* (1998) in sensitivity experiments with the objective to mimic complex GCM (ECHAM) CO_2-scenario climates and their atmospheric variability with an adapted simplified GCM (PUMA).

(b) Given the variability of a recurrent large scale atmospheric flow pattern, the heating is determined, which generates the growth or decay of these patterns on timescales of the order of ten days. We demonstrate the use of adjoint modelling diagnostics based on the PUMA-GCM to derive the forcing of the observed variability.

Oortwijn and Barkmeijer (1995) employ the adjoint of a quasi-geostrophic three layer model to determine perturbations that optimally enhance the projection of the atmospheric state on a blocking pattern at forecast time. Corti and Palmer (1997) apply the same type of model to investigate the sensitivity of the NAO and PNA-pattern to small streamfunction perturbations. Adjoint model diagnostics allows the direct identification of location, shape, and magnitude of the sensitive regions (Hall 1986). Here we modify this technique and look for perturbations of the heating in PUMA and demonstrate a sensitivity study in an idealised setting.

The outline of the study is as follows. First the PUMA model and its adjoint are introduced. Section 3 demonstrates the reconstrucion of the forcing from the mean climate response. In section 4 the detection of the temperature forcing of climate variability, given by a daily NAO-index, is illustrated in an idealised setting.

22.2 PUMA and its adjoint

The PUMA model solves the primitive equations on a sphere with optional orography (Hoskins and Simmons 1975), but it is completely recoded in Fortran 90 with some alterations (Fraedrich *et al.* 1998). Due to its portable and transparent coding it is used for research and educational purposes. Rayleigh friction at the lowest level and Newtonian cooling are the only parameterisations. The Newtonian cooling parameterisation for the diabatic forcing uses a relaxation temperature field T_R. At each timestep the model temperature T is relaxed towards this parameter with a time constant $\tau(\sigma)$:

$$\left(\frac{\partial T}{\partial t}\right)_{diabatic} = \frac{T_R - T}{\tau(\sigma)}. \tag{22.1}$$

Physically the relaxation temperature T_R can be interpreted as a radiative-convective equilibrium temperature. Due to advection there are significant differences between the relaxation temperature field and the time mean temperature of the model. For the experiments presented here the resolution is set to five σ-levels in the vertical with the highest level centered at 100 hPA and approximately $5.6° \times 5.6°$ (T21) in the horizontal. The time step is set to one hour. The relaxation time constant is set to five days at the lowest, ten days at the second lowest, and thirty days at the other levels. The model has been used in a number of studies ranging from ultra-low-frequency variability (James *et al.*

1994) to storm track organisation (Frisius *et al.* 1998), storm track interaction (Franzke *et al.* 2000), low frequency variability and teleconnections (Franzke *et al.* 2001), storm track sensitivity towards SST anomalies (Walter *et al.* 2001), and climate change scenarios (Lunkeit *et al.* 1998).

Adjoint PUMA model: The adjoint PUMA model is derived by the Tangent and Adjoint Model Compiler (TAMC; Giering and Kaminski 1996, 1998, Giering 1999). Since adjointness is a property of linear operators, the adjoint model is, strictly speaking, adjoint to the tangent linear version of PUMA. It describes the linear growth of a perturbation of the nonlinearly evolving flow. Therefore, a tangent linear model can be written as a linear operator, which depends nonlinearly on the unperturbed flow. Since there is no feedback from the perturbation to the unperturbed flow, it can extract an infinite amount of energy violating the energy conservation. Consequently simulations with the tangent linear model are only valid for short time periods of the order of a few days.

Let $\mathbf{A}$ be a matrix representing the tangent linear operator for a given flow and time period. Then its adjoint $\mathbf{A}^*$ is defined by

$$(\mathbf{A}x, y) = (x, \mathbf{A}^* y)\,, \tag{22.2}$$

where $(\cdot, \cdot)$ is an inner product and not necessarily Euclidian. With complex x and y the operator $\mathbf{A}^*$ is the Hermitian or conjugate transpose $\mathbf{A}^*$ of $\mathbf{A}$; for real x and y this is just the transpose. The adjoint operator $\mathbf{A}^*$ is useful in a number of calculations. If it exists as a model code, various states can be analysed without extracting the matrix $\mathbf{A}$ for each case individually, which is time consuming. The choice of x and y is subject to definition. They may, for instance, be streamfunction disturbances at different times, but many other choices are useful depending on the application. An introduction to adjoint applications can be found for instance in Errico (1997) or Talagrand (1991) while Marchuk (1974) is probably the first source that applies adjoint methods in meteorology.

22.3 Tuning: Forcing of a mean state

Aims and Methods: The long-term or climate mean fields are considered as the response to a forcing. In particular, changes in the climate are linked to changes in the climate forcing. Here we analyse the link from a time-mean temperature field (target climate $\overline{T}_T$ from the control run) to its forcing field. That is, a suitable forcing field is reconstructed (for example, the PUMA relaxation temperature T_R), whose time-mean response (substitute climate $\overline{T}$) should be as close to the target climate $\overline{T}_T$, as possible. A unique forcing-response relation, however, cannot always be guaranteed as different forcings may lead to the same climate mean state. Therefore we carry out an internal experiment in the sense that the target climate itself has been produced by the PUMA with a prescribed forcing.

This allows an objective judgement of the quality of the forcing reconstruction by comparison with the known solution. For the forcing reconstruction we define a cost function J, which describes the distance between target and its substitute:

$$J := \frac{1}{2}\left(\overline{T} - \overline{T}_T, \overline{T} - \overline{T}_T\right). \tag{22.3}$$

In the experiments discussed here the inner product $(\cdot,\cdot)$ contains area weights to compensate for the geometry of the model grid and variance scaling with the temperature variance of the control run. For the forcing reconstruction this cost function needs to be minimised by choice of appropriate parameters T_R of the relaxation temperature. The gradients of J with respect to the parameters are calculated by the adjoint PUMA. Let $\mathcal{H}$ be the mapping of the $n \,\epsilon\, \mathbb{N}$ parameters T_R on the n elements of $\overline{T}$ as calculated by PUMA:

$$\begin{aligned} \mathcal{H} : \mathbb{R}^n &\rightarrow \mathbb{R}^n \\ T_R &\mapsto \overline{T}. \end{aligned} \tag{22.4}$$

This makes the cost function J and its first order approximation δJ:

$$J(T_R) = \frac{1}{2}\left(\mathcal{H}(T_R) - \overline{T}_T, \mathcal{H}(T_R) - \overline{T}_T\right) \tag{22.5}$$

$$\delta J = \left(\nabla_{T_R} J(T_R), \delta T_R\right). \tag{22.6}$$

This equation introduces the gradient operator with respect to the parameters of the relaxation temperature field ∇_{T_R} to relate a small perturbation of this parameter δT_R to a change in the cost function δJ. Let $A\,|_{T_{R_0}}$ be the tangent-linear model of $\mathcal{H}$, which is the Jacobian of $\mathcal{H}$ at a first-guess relaxation temperature field T_{R_0}. By writing $\delta\overline{T} = A\big|_{T_{R_0}} \delta T_R$, the differentiation of (22.5) and subsequent application of the adjoint model A^* (22.2) yields:

$$\delta J = \left(\mathcal{H}(T_{R_0}) - \overline{T}_T, A\big|_{T_{R_0}} \delta T_{R_0}\right) \tag{22.7}$$

$$= \left(A^*\big|_{T_{R_0}} \left(\mathcal{H}(T_{R_0}) - \overline{T}_T\right), \delta T_R\right). \tag{22.8}$$

Comparing (22.8) with the definition of the gradient of the cost function $\nabla_{T_R} J(T_{R_0})$ (22.6) leads to:

$$\nabla_{T_R} J(T_{R_0}) = A^*\big|_{T_{R_0}} \left(\mathcal{H}\left(T_{R_0}\right) - \overline{T}_T\right). \tag{22.9}$$

The linear operators $A\,|_{T_{R_0}}$ and $A^*\,|_{T_{R_0}}$ represent the tangent linear model and its adjoint. Both depend on the first guess relaxation temperature field T_{R_0} about which the model is linearised. Equation (22.9) shows how the gradient of the cost function with respect to the relaxation temperature parameters can be calculated efficiently by feeding the misfit between the calculated and the targeted time mean model temperature, $\mathcal{H}(T_{R_0}) - \overline{T}_T$, into the adjoint model $A^*\,|_{T_{R_0}}$.

Single stormtrack climate (control run): Reconstructing the forcing of the mean climate we use a single stormtrack climate (Frisius *et al.* 1998). It is generated by a meridionally oriented heating and cooling dipole of the relaxation temperature T_R (Fig. 22.2a), representing the contrast between a cold continent and a warm ocean current. In the vertical its amplitude follows a lapse rate and becomes isothermal near the tropopause. The climate response is characterised by a stormtrack developing downstream of the heating dipole. We use the climate mean temperature $\overline{T}$ (Fig. 22.2b) of this model climate (and its standard deviation σ_T; Fig. 22.2c) as the target climate $\overline{T}_T$ to reconstruct the forcing T_R.

Cost function properties: Experience has shown that with the above type of cost function, where the time average of a variable is included, a few precautions need to be taken. Lea *et al.* (2000) investigate the dependence of a time averaged variable of the Lorenz (1963) model on a single parameter. Their results suggest that analytical gradients calculated with the adjoint model are not useful for minimising the cost function when the averaging time is too long. Nonlinear dependence of the cost function on the parameter lets the gradient attain too large values which only represent the slope in a very small neighbourhood. On the other hand, for short averaging times, the dependence on the initial conditions of the model variables distorts the picture. Therefore, they suggest an ensemble of adjoint gradient calculations, with different initialisations of the model variables and an intermediate averaging time. In the PUMA model the shape of the cost function depends on the high-dimensional relaxation temperature field. In order to plot the cost function for the PUMA model against the averaging time and the choice of the relaxation temperature (Fig. 22.1), it is made dependent on a single parameter λ which represents a one-dimensional parameter subspace:

$$T_R = (1 - \lambda)\overline{T}_T + \lambda T_{R_0}. \tag{22.10}$$

Here T_{R_0} is chosen to be the relaxation temperature of the control experiment, which is the forcing of the single stormtrack climate. Choosing the mean temperature response as the target climate $\overline{T}_T$ in the cost function J, we expect J to converge towards zero for $\lambda = 1$ and $t \to \infty$.

Indeed the cost function possesses a marked minimum, where the forcing has the right shape and amplitude ($\lambda = 1$) even for short averaging times. This justifies the choice of an averaging time of 240 timesteps for the cost function in the gradient calculations. At intermediate times in the order of months, however, internal variability causes some shifting of the minimum without severely changing its location.

Forcing reconstruction: An internal experiment is carried out to reconstruct the forcing of the single stormtrack climate. The mean temperature distribution of the control run (Fig. 22.2b) is taken as the target climate $\overline{T}_T$ in the cost function J. An iterative algorithm is used: First an ensemble of five calculations of the

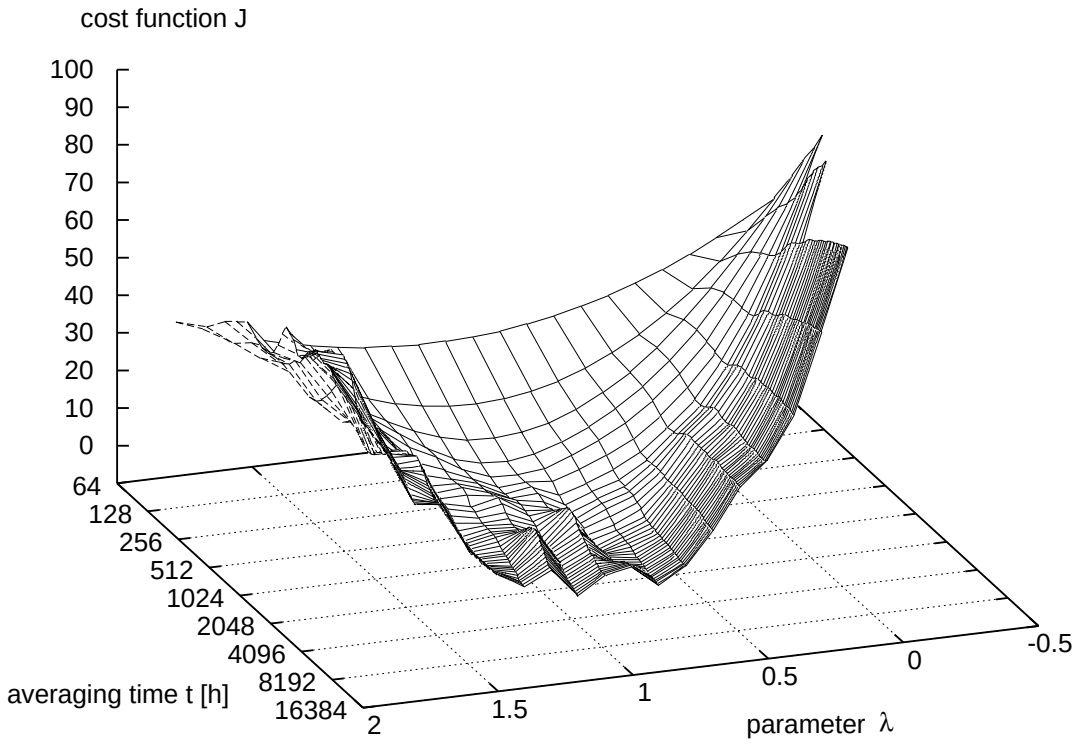

Figure 22.1: Cost function depending on different averaging times and parameters. The relaxation temperature parameters T_R change from the target mean temperature $\overline{T}_T$ ($\lambda = 0$) to the known relaxation temperature of the control run T_{R_0} ($\lambda = 1$) as described by equation (22.10). All integrations start ($t = 0$) from the same atmospheric state randomly chosen from the control run.

gradient is carried out with an averaging time of 240 timesteps (corresponding to ten days). The initial conditions of the next ensemble member are the final conditions of its predecessor. The ensemble mean gradient field is then used to alter the relaxation temperature field T_R (that is the forcing) by a small amount. Subsequently the model is run for 1200 time steps (50 days) to let the circulation adapt to the new parameters; then the cost function is evaluated. The final atmospheric conditions are made the initial conditions of the next iteration. The procedure is repeated until there is no further decrease of the cost function.

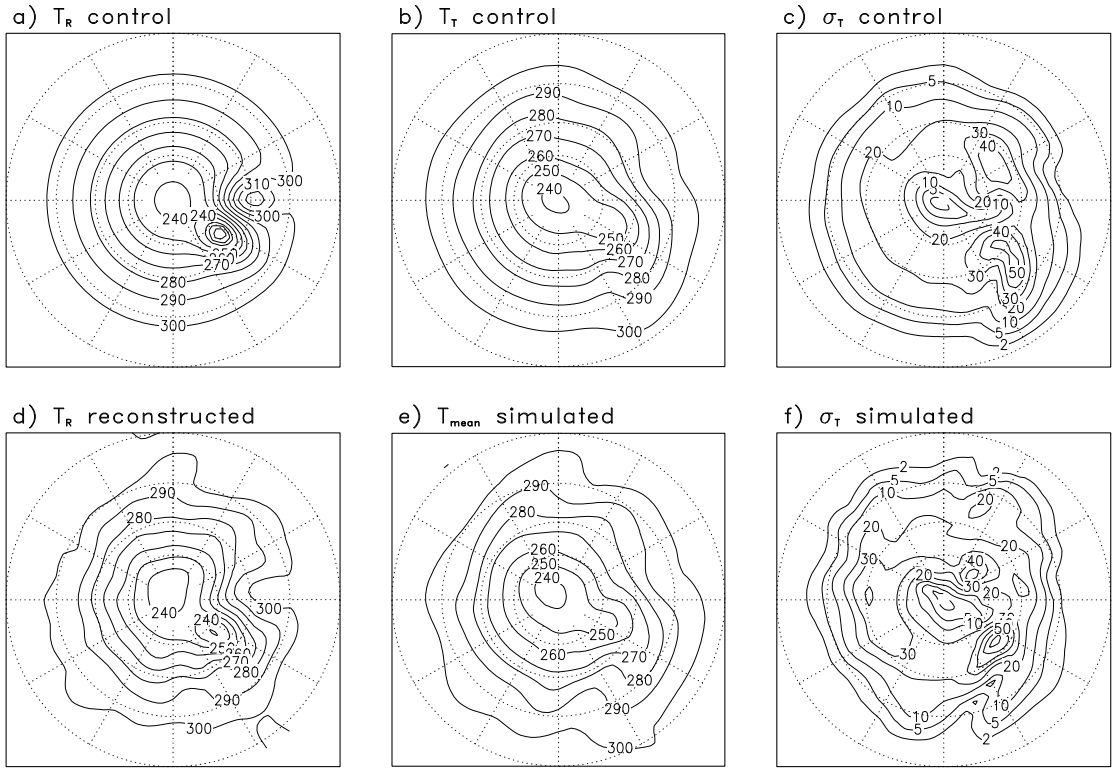

Figure 22.2: *Control run (single stormtrack climate):* a) Relaxation temperature T_{R_0}, b) mean temperature $\overline{T}$ and target temperature $\overline{T}_T$ in the cost function J, c) standard deviation of the temperature σ_T. *Reconstruction:* d) Relaxation temperature T_R reconstructed from $\overline{T}_T$, e) mean temperature of a simulation with T_R, f) standard deviation of the temperature in the simulation with relaxation temperature T_R (all at σ-level 0.9 near 900 hPa).

Results: The gradients of the cost function J, obtained by the adjoint model and applied to reconstruct the single stormtrack climate of the control run, determine the forcing reasonably well in the lower levels of the model (Fig. 22.2d) while

the upper levels (not shown) are less well defined. The relaxation time constant $\tau(\sigma)$ (Eq. 22.1) is larger in the upper (30 days) than in the lower levels (10 and 5 days, respectively). They reflect the relative importance of advection versus radiative forcing. Long relaxation timescales should make the problem more nonlinear. However shorter relaxation times in the upper layers cannot be seen as a remedy since they would make the model less realistic and consequently alter the link between climate and forcing.

A PUMA simulation with the reconstructed relaxation temperature T_R leads to a time mean temperature (Fig. 22.2e), which is remarkably similar to the mean temperature distribution of the control run ($\overline{T}_T$). This is also true for the upper levels and in contrast to the poor reconstruction of the forcing in these levels. Again their longer relaxation timescale appears to be the reason but this time with a positive effect. Baroclinic processes probably triggered by the bottom level make up for the errors in the radiative-convective parameterisation in the temperature tendency. The similarities between the temperature variances in the control run (Fig. 22.2c) and the simulation (Fig. 22.2f) are less well pronounced but some features are reproduced. A second experiment, which includes orography in the control run and in the run with the reconstructed forcing, yields results of comparable quality (not shown).

22.4 Detection: Forcing of variability

Aims and methods: Short-term processes are part of the space-time climate variability. Their sensitivity to small changes of the forcing may contribute substantially to the climate sensitivity. For example, a daily NAO-index and its changes are linked to an atmospheric forcing and its modification.

Low-frequency variability in PUMA: The interaction of two stormtracks of 150° zonal distance reveals patterns, which are similar to the NAO and the PNA (Franzke *et al.* 2001). They are introduced into the model by two heating dipoles in the manner described for the control climate of the previous chapter. This stormtrack separation defines a larger A-region and a smaller P-region which have the approximate meridional extent of an 'Atlantic' and 'Pacific' region separated by the North American east cost and Japan. The A-pattern ψ_A (Fig. 22.3) is the one-point correlation from the basepoint 47°N, 56°W in the A-region. We define a daily NAO-type or A-index $\mathcal{I}$ by projection of the local streamfunction anomaly of the daily streamfunction ψ_d from the mean $\overline{\psi}$ on this pattern.

$$\mathcal{I}(\psi_d) = \frac{\langle \psi_d - \overline{\psi}, \psi_A \rangle}{|\psi_A|}. \tag{22.11}$$

The brackets $\langle \cdot, \cdot \rangle$ denote a scalar product with area weighting which compensates for the the geometry of the model grid. For the detection of the variability forcing

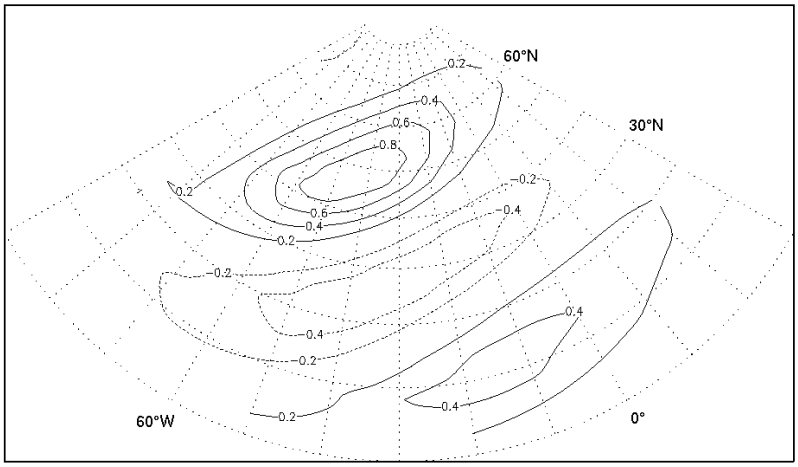

Figure 22.3: *One-point correlation in the A-region with basepoint* $47°N$, $56°W$ *(from Franzke et al. 2001). This pattern is referred to as the A-pattern* ψ_A.

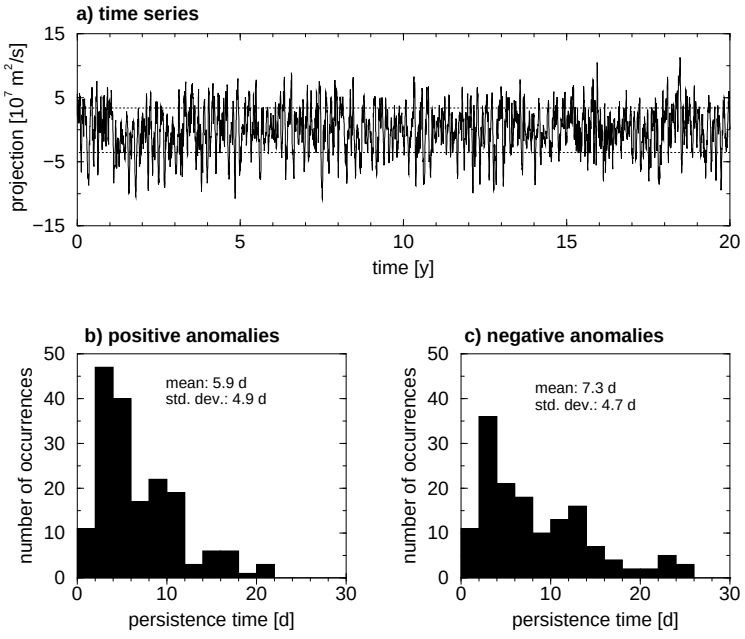

Figure 22.4: A-Index (projection of the streamfunction on the A-Pattern): a) Time series of 20 years (7200 days; one standard deviation dotted) and histogram of persistence times of b) positive and c) negative projections exceeding one standard deviation.

(section 22.4) a time series of the daily index is calculated for a 20 year period (Fig. 22.4a). Anomalies exceeding one standard deviation show persistence of up to 25 days (Fig. 22.4b and c); the negative anomalies tend to last longer than the positive ones. We select special events in this A-index timeseries and calculate their associated temperature sensitivity patterns which lead to its increase when introduced into the model as perturbations. Adjoint modelling provides an advanced diagnostic tool to quantify this forcing-response sensitivity without rerunning a suite of complex GCM experiments with different initial conditions. The adjoint model directly calculates the spatial sensitivity patterns which, in a first order approximation, most effectively induce a given change in the output. Here we define the PUMA model to be a mapping $\mathcal{H}$ of the temperature $T(-t)$ at time $-t$ on streamfunction $\psi(0)$ at time 0:

$$\begin{aligned} \mathcal{H} : \mathbb{R}^n &\rightarrow \mathbb{R}^n \\ T(-t) &\mapsto \psi(0). \end{aligned} \tag{22.12}$$

This allows us to write the A-index $\mathcal{I}(\psi_d(0))$ (Eq. 22.11) at time 0 as a function of the temperature $T(-t)$ at time $-t$:

$$\mathcal{I}(\psi_d(0)) = \frac{\langle \mathcal{H}(T(-t)) - \overline{\psi}, \psi_A \rangle}{\|\psi_A\|} \tag{22.13}$$

$$\Rightarrow \delta\mathcal{I} = \frac{\langle R(-t,0)\delta T(-t), \psi_A \rangle}{\|\psi_A\|}, \quad with \quad \delta\psi(t) = R(-t,0)\delta T(-t) \tag{22.14}$$

$$= \frac{\langle \delta T(-t), R^*\psi_A \rangle}{\|\psi_A\|}. \tag{22.15}$$

Introduction of the tangent-linear propagator $R(-t,0)$ (the linearisation of $\mathcal{H}$) yields equation (22.14) for the first order approximation of the A-index $\delta\mathcal{I}$, and application of its adjoint propagator R^* (Eq. 22.2) gives equation (22.15). It follows that, in order to have a maximum change $\delta\mathcal{I}$ of the A-index $\mathcal{I}$ at time 0, the initial temperature perturbation $\delta T(-t)$ needs to have maximum projection on $R^*\psi_A/\|\psi_A\|$, which, therefore, is interpreted as the sensitivity pattern. Keeping the norm of the temperature, $\|\delta T(-t)\|$, fixed, we see that the sensitivity pattern $R^*\psi_A/\|\psi_A\|$ in equation (22.15) not only defines the spatial shape but also the strength of the sensitivity of the index change $\delta\mathcal{I}$ on the initial temperature perturbation $\delta T(-t)$.

Sensitivity of the A-Index: Two special states of the A-index $\mathcal{I}$ are analysed. They are defined by at least five days of continuous index growth beyond plus (minus) one standard deviation. The sensitivity patterns $R^*\psi_A/\|\psi_A\|$ are calculated for different lag times $-t$ of 1 to 4 days. The composite pattern for each lag time is the average of 34 (46) cases found in the A-index time series (Fig. 22.4a). In addition the presence of the sensitivity patterns in the actual model run is verified

by calculating lag correlations between the projection of the model temperature onto the sensitivity patterns and the A-index time series.

Results: The composite sensitivity patterns for the cases with a growing positive A-index anomaly (Fig. 22.5) show a wave-like structure that propagates more and more upstream with increasing lag time. In the vertical there is an increasing westward tilt from equivalent barotropic in the 24 h pattern to a clearly baroclinic structure in the 96 h pattern. The composite sensitivity patterns of growing positive and growing negative (not shown) A-index anomalies are quite similar. The lag correlations between the projection of the model temperature on the composite temperature sensitivity patterns and the 20-year index time series are quite strong (Fig. 22.6). They peak close to the lag time corresponding to the sensitivity pattern, which underlines the dynamical importance of the detected patterns. The cases for the growth of negative A-index are similar (not shown). The correlations are different from zero on the 99.9% level. It is not obvious, however, whether positive anomalies in the projection on the temperature patterns correlate with positive index anomalies or whether mainly the respective negative anomalies are correlated. When computing only positive and negative projections in the lag correlation, their relative contributions are of almost equal importance as expected for a linear mechanism. This is in good agreement with the similarity of the patterns for the two situations. The largest correlation, however, appears closer to lag zero than expected. This shift again does not depend on the sign of the respective temperature anomaly. By correlating the projection on each individual model level we find that the shift of the maximum is strongest in the contribution of the lower levels and not present in the 300 hPa-level.

22.5 Summary and conclusions

Reconstructing past climate states requires the identification of the climate mean state and the climate variability of the atmosphere and, once interpreted as a response, the type of the underlying atmospheric forcing. How adjoint modelling may contribute to this goal, is demonstrated by a GCM approach to reconstruct the forcing of the climate mean *and* to diagnose the forcing of the climate variability. Given the climate mean, the associated location, shape and intensity of the forcing can be successfully determined so that, with this reconstruction, both the climate mean and its variability are retained.

As first example for this feasibility study we choose the single stormtrack climate simulated by an idealised experiment with the simplified general circulation model PUMA. The reconstruction of the forcing from a climate mean response may be useful for two main types of experiments: Firstly, adaptation of the model forcing to complex GCM climates (for instance with ocean coupling) allows the isolated investigation of the internal variability of the atmosphere and, due to the

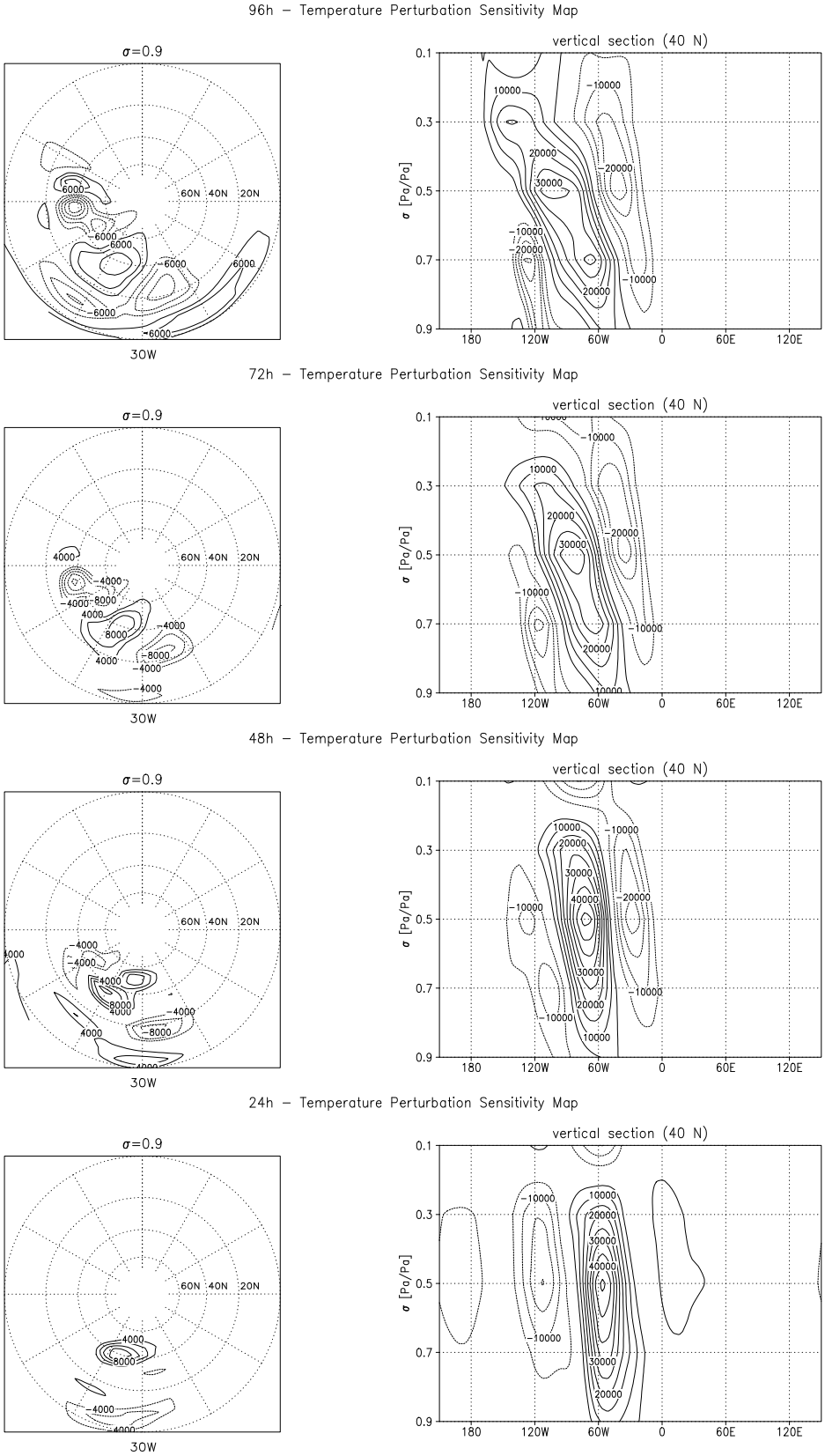

Figure 22.5: Composite temperature sensitivity patterns for the positive A-index growth cases (from top to bottom: 96 h, 72 h, 48 h, and 24 h; units are $m^2 s^{-1} K^{-1}$).

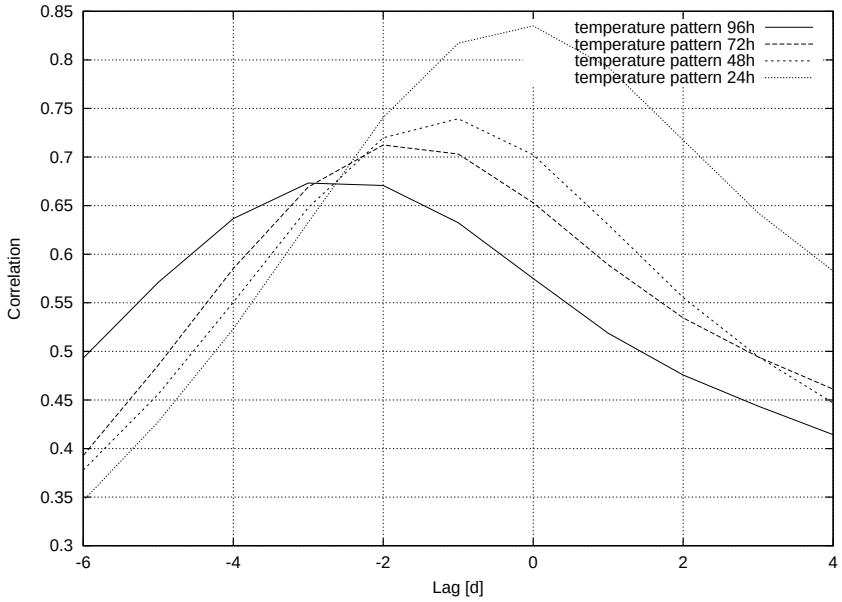

Figure 22.6: Lag correlation between the projection on the temperature sensitivity patterns (growth cases) and the A-index time series. Negative lag times mean leading temperature pattern.

relatively higher integration speed of the simplified model, longer runs and, therefore, better statistics. Secondly, climate reconstruction from temperature maps derived from suitable proxy data may give an dynamically consistent estimate of other climate variables and their variability which is not so easily obtained from proxy data. The method as presented here is limited to scenarios with constant forcing. Another limitation arises from the uncertainty of the reconstruction in the upper model levels which appears to be a consequence of the strong advective component of the temperature tendencies at these levels. This may be related to the question of the uniqueness of the solution which cannot be guaranteed.

Given the climate variability, the forcing of a large scale atmospheric teleconnection pattern on short timescales is diagnosed. We choose the North Atlantic Oscillation, which determines Europe's present and past climates. It has also been simulated by an idealised GCM experiment (PUMA). We determine those temperature sensitivity patterns, which generate a NAO-index increase. The diagnosed temperature sensitivity patterns may help to identify mechanisms, which force the variability of large scale atmospheric teleconnection patterns. Forcing the model with one of the sensitivity patterns leads to a significant change of the probability density function of the NAO-Index, which is consistent with results from Corti and Palmer (1997). By identifying directly the heating sensitivity patterns in a primitive equations model we may achieve a better understanding of how the atmosphere reacts on changes of the forcing. It is a tool to determine the influence of a (possibly external) thermal forcing on internal atmospheric

variability. The reversed approach by the adjoint technique reveals sensitivities not previously considered which is in contrast to the direct method where perturbations are introduced in a more or less systematic way and therefore are shaped by the initial paradigm. The main limitation lies in the linearity of the adjoint sensitivities. Their validity is depending on the linearity of the studied process which in turn determines the timescale. For the atmosphere this results in the order of 10 days at maximum. However this is enough for some of the dynamical processes linked with persistent large scale atmospheric circulation patterns taken into account that tangent-linearity allows for the calculation of first order sensitivities along almost arbitrarily complex trajectories.

These results suggest that the adjoint techniques presented may be successfully applied to analyse palaeoclimates by reconstructing and diagnosing the atmospheric forcing, which generates the atmospheric mean state, its variability, and the underlying processes. Other adjoint techniques found in the literature, such as the characterisation of the background flow by its (scalar) overall sensitivity (Oortwijn and Barkmeijer 1995), or the stability analysis of persistent states by finite time fastest growing modes (Frederiksen 2000), may also prove useful in the field of palaeoclimatology.

Acknowledgements

Financial support was provided by the Bundesministerium für Bildung und Forschung (BMBF, Förderkennzeichen 01LG9907, "Die atmosphärische Variabilität in Abhängigkeit von Schwankungen des solaren Antriebs auf Zeitskalen bis zu 10.000 Jahren") as an accompanying study to the strategy fund project "Natural climate variations from 10,000 years BP to the present day" (Klima in historischen Zeiten, KIHZ) of the Helmholtz Association of German Research Centres; C. Franzke supplied the data.

Bibliography

Appenzeller, C., T. Stocker, and M. Anklin, 1998: North atlantic oscillation dynamics recorded in greenland ice cores. *Science*, **282**(5388), 446 – 449.

Corti, S. and T. Palmer, 1997: Sensitivity analysis of atmospheric low-frequency variability. *Quart. J. Roy. Meteor. Soc.*, **123**(544), 2425 – 2447.

Errico, R. M., 1997: What is an adjoint model? *Bull. Amer. Meteor. Soc.*, **78**(11), 2577–2591.

Fraedrich, K., E. Kirk, and F. Lunkeit, 1998: Portable University Model of the Atmosphere. Technical Report **16**, DKRZ, 37 S.

Franzke, C., K. Fraedrich, and F. Lunkeit, 2000: Low frequency variability in a simplified atmospheric global circulation model: Storm track induced 'spatial resonance'. *Quart. J. Roy. Meteor. Soc.*, **126**, 2691–2708.

Franzke, C., K. Fraedrich, and F. Lunkeit, 2001: Teleconnections and low-frequency variability in idealized experiments with two storm tracks. *Quart. J. Roy. Meteor. Soc.*, **127**(574), 1321 – 1339.

Frederiksen, J., 2000: Singular vectors, finite-time normal modes, and error growth during blocking. *J. Atmos. Sci.*, **57**, 312 – 333.

Frisius, T., F. Lunkeit, K. Fraedrich, and I. James, 1998: Storm-track organization and variability in a simplified atmospheric global circulation model. *Quart. J. Roy. Meteor. Soc.*, **124**(548), 1019 – 1043.

Giering, R., 1996: *AMC: Ein Werkzeug zum automatischen Differenzieren von Fortran-Programmen*, vol. 42 of *Forschung und wissenschaftliches Rechnen, Beiträge zum Heinz-Billing-Preis 1995*. Gesellschaft für wissenschaftliche Datenverarbeitung mbH, Göttingen, Germany, 11-27.

Giering, R., 1999: *Tangent linear and Adjoint Model Compiler, Users manual 1.4*. [http://puddle.mit.edu/~ralf/tamc].

Giering, R. and T. Kaminski, 1998: Comparison of automatically generated code for evaluation of first and second order derivates to hand written code from the

Minpack-2 collection. *Automatic Differentiation for adjoint code generation*, Faure, C., ed., vol. 3555. INRIA.

Hall, M., 1986: Application of adjoint sensitivity theory to an atmospheric general-circulation model. *J. Atmos. Sci.*, **43**(22), 2644–2651.

Hoskins, B. J. and A. J. Simmons, 1975: A multi-layer spectral model and the semi-implicit method. *Quart. J. Roy. Meteor. Soc.*, **101**, 637–655.

James, P. M., K. Fraedrich, and I. N. James, 1994: Wave-zonal-flow interaction and ultra-low-frequency variability in a simplified global circulation model. *Quart. J. Roy. Meteor. Soc.*, **120**, 1045–1067.

Jones, J. M. and M. Widmann, 2004: Reconstructing large-scale variability from palaeoclimatic evidence by menas of data assimilation through upscaling and nudging (DATUN). *The KIHZ project: Towards a Synthesis of Holocene Proxy Data and Climate Models*, Fischer, H., Kumke, T., Lohmann, G., Flser, G., Miller, H., von Storch, H., and Negendank, J. F. W., eds.. Springer, Berlin Heidelberg New York, 171-193.

Lea, D. J., M. R. Allen, and T. W. Haine, 2000: Sensitivity analysis of the climate of a chaotic system. *Tellus*, **52A**, 523 – 532.

Li, Z., A. Barcilon, and I. Navon, 1999: Study of block onset using sensitivity perturbations in climatological flows. *Mon. Weather Rev.*, **127**, 879 – 900.

Li, Z. and L. Ji, 1997: Efficient forcing and atmospheric teleconnections. *Q. J. R. Meteorol. Soc.*, **123**(544), 2401 – 2423.

Lorenz, E. N., 1963: Deterministic nonperiodic flow. *J. Atmos. Sci.*, **20**, 130–141.

Lunkeit, F., K. Fraedrich, and S. E. Bauer, 1998: Strom tracks in a warmer climate: sensitivity studies with a simplified global circulation model. *Climate Dynamics*, vol. 14. Springer-Verlag, 813-826.

Marchuk, G. I., 1974: *Numerical Solution of Problems in Atmospheric and Oceanic Dynamics.* Gidrometeoizdat, Leningrad, 304. (in Russian).

Oortwijn, J., 1999: Growth properties of optimal transition perturbations. *J. Atmos. Sci.*, **56**, 2491 – 2511.

Oortwijn, J. and J. Barkmeijer, 1995: Perturbations that optimally trigger weather regimes. *J. Atmos. Sci.*, **52**(22), 3932–3944.

Raible, C., U. Luksch, K. Fraedrich, and R. Voss, 2001: North Atlantic decadal regimes in a coupled GCM simulation. *Clim. Dyn.*, **18**, 321–330.

Talagrand, O., 1991: The use of adjoint equations in numerical modeling of the atmospheric circulation. *Automatic Differentiation of Algorithms: Theory, Implementation, and Application*, Griewank, A. and Corlies, G., eds.. SIAM, 169-180.

von Storch, H., U. Cubasch, J. F. Gonzales-Rouco, J. M. Jones, R. Voss, M. Widmann, and E. Zorita, 2000: Combining paleoclimatic evidence and GCMs by means of data assimilation through upscaling and nudging (DATUN). *11th Symposium on global change studies*, AMS, Long Beach, CA., 28–31.

Walter, K., U. Luksch, and K. Fraedrich, 2001: A response climatology of idealised midlatitude SST anomaly experiments with and without stormtrack. *J. Climate*, **14**, 467–484.